

# Evolution of rarefaction pulses into vortex rings.

Natalia G. Berloff

Department of Mathematics

University of California, Los Angeles, CA, 90095-1555

*nberloff@math.ucla.edu*

(November 19, 2018)

The two-dimensional solitary waves of the Gross-Pitaevskii equation in the Kadomtsev-Petviashvili limit are unstable with respect to three-dimensional perturbations. We elucidate the stages in the evolution of such solutions subject to perturbations perpendicular to the direction of motion. Depending on the energy (momentum) and the wavelength of the perturbation different types of three-dimensional solutions emerge. In particular, we present new periodic solutions having very small energy and momentum per period. These solutions also become unstable and this secondary instability leads to vortex ring nucleation.

Considerable interest is attached to determining the entire solitary wave sequences of solutions of the Gross-Pitaevskii (GP) model [1] because they define possible states that can be excited in a Bose condensate. Jones and Roberts [2] determined the entire sequence of solitary solutions numerically for the GP model  $-2i\psi_t = \nabla^2\psi + (1 - |\psi|^2)\psi$ , where we use dimensionless variables such that the unit of length corresponds to the healing length  $a$ , the speed of sound is  $c = 1/\sqrt{2}$ , and the density at infinity is  $\rho_\infty = 1$ . The solitary wave solutions satisfy two conditions: (1) the disturbance associated with the wave vanishes at large distances:  $\psi \rightarrow 1$ ,  $|\mathbf{x}| \rightarrow \infty$  and (2) they preserve their form as they propagate with a dimensionless velocity  $U$ , so that  $\psi(x, y, z, t) = \psi(x', y, z)$ ,  $x' = x - Ut$ , in three dimensions (3D) and  $\psi(x, y, t) = \psi(x', y)$ , in two dimensions (2D), so that the solitary wave solutions satisfy

$$2iU \frac{\partial \psi}{\partial x'} = \nabla^2 \psi + (1 - |\psi|^2)\psi. \quad (1)$$

Jones and Roberts calculated the energy  $\mathcal{E}$  and momentum  $\mathcal{P}$  given by

$$\mathcal{E} = \frac{1}{2} \int |\nabla \psi|^2 dV + \frac{1}{4} \int (1 - |\psi|^2)^2 dV \quad (2)$$

$$\mathcal{P} = \frac{1}{2i} \int [(\psi^* - 1)\nabla \psi - (\psi - 1)\nabla \psi^*] dV, \quad (3)$$

and determined the location of the sequence on the  $\mathcal{P}\mathcal{E}$ -plane.

In three dimensions they found two branches meeting at a cusp where  $\mathcal{P}$  and  $\mathcal{E}$  assume their minimum values,  $\mathcal{P}_{\min}$  and  $\mathcal{E}_{\min}$ . As  $\mathcal{P} \rightarrow \infty$  on each branch,  $\mathcal{E} \rightarrow \infty$ . On the lower branch the solutions are asymptotic to large vortex rings.

As  $\mathcal{E}$  and  $\mathcal{P}$  decrease from infinity along the lower branch, the solutions begin to lose their similarity to large vortex rings. Eventually, for a momentum  $\mathcal{P}_0$  slightly

greater than  $\mathcal{P}_{\min}$ , they lose their vorticity ( $\psi$  loses its zero), and thereafter the solitary solutions may better be described as ‘rarefaction waves’. The upper branch consists entirely of these and, as  $\mathcal{P} \rightarrow \infty$  on this branch, the solutions asymptotically approach the rational soliton solution of the Kadomtsev-Petviashvili Type I (KPI) equation [3] and are unstable. In 2D the family of the solitary wave solutions are represented by two point vortices if  $U \leq 0.4$ . As the velocity increases the wave loses its vorticity and becomes a rarefaction pulse. As  $U \rightarrow 1/\sqrt{2}$  both the energy,  $\mathcal{E}$  and momentum  $\mathcal{P}$  per unit length approach zero and the solutions asymptotically approach the 2D rational soliton solution of KPI.

Jones and Roberts [2] derived the KPI equation using an asymptotic expansion in the parameter  $\epsilon^2 \approx 2(1 - \sqrt{2}U)$ , which is small when  $U$  approaches the speed of sound. They sought solutions of the form  $\psi = f + ig$ , where  $f = 1 + \epsilon^2 f_1 + \epsilon^4 f_2 + \dots$ ,  $g = \epsilon g_1 + \epsilon^3 g_2 + \dots$ ,  $U = 1/\sqrt{2} + \epsilon^2 U_1 + \dots$ . The independent variables were stretched, so that  $\xi = \epsilon x'$ ,  $\eta = \epsilon^2 y$ , and  $\zeta = \epsilon^2 z$ . By substituting these expressions into (1) and considering real and imaginary parts at the leading and first orders in  $\epsilon$ , they determined that  $g_1$  satisfies the KPI equation:

$$\frac{\partial^2 g_1}{\partial \xi^2} + \nabla_{\eta\zeta}^2 g_1 - \frac{\partial}{\partial \xi} \left[ \frac{1}{2} \frac{\partial^3 g_1}{\partial \xi^3} - \frac{3}{\sqrt{2}} \left( \frac{\partial g_1}{\partial \xi} \right)^2 \right] = 0, \quad (4)$$

and  $f_1 = \partial g_1 / \sqrt{2} \partial \xi - g_1^2$ ,  $U_1 = -1/2\sqrt{2}$ . In 2D the equation (4) has a closed form solution [4], so that the asymptotic solution of the GP equation in the KPI limit is

$$\psi = 1 - i \frac{2\sqrt{2}x'}{x'^2 + \epsilon^2 y^2 + 3/2\epsilon^2} - \frac{2}{x'^2 + \epsilon^2 y^2 + 3/2\epsilon^2}, \quad (5)$$

which we have written in the original variables.

It was shown by Kuznetsov and Turytsin [5] that the 2D KPI soliton is stable to 2D but unstable to 3D perturbations. The linear stability analysis of 2D solitary

solution of the GP equation subject to long wavelength infinitesimal perturbations was done by Kuznetsov and Rasmussen [6]. They demonstrated that all long wavelength antisymmetric modes are stable and all long wavelength symmetric modes are unstable. In particular they showed that the growth rate of symmetric perturbations,  $\sigma$ , is given by  $\sigma^2 = -\mathcal{E}k^2/(\partial\mathcal{P}/\partial U) > 0$ , as the wavenumber  $k \rightarrow 0$ . The maximum growth rate of instability and the instability region of 2D solitary solutions were found in [7] by solving the linear stability problem. Through numerical integration of the GP equation it was shown that as perturbations grow to finite amplitude the vortex lines reconnect to produce a sequence of almost circular vortex rings. Senatorski and Infeld [8] numerically integrated the KPI equation to study the fate of 2D KPI solitons subject to 3D perturbations. They determined that 2D KPI solitons evolve into 3D KPI solitons which are also unstable.

The goal of this Letter is to elucidate the fate of the 2D rarefaction pulse in the KPI limit of the GP model subject to 3D perturbations. We discovered that such solutions may evolve into vortex rings and this establishes a new mechanism of vortex nucleation. We found that this mechanism can operate in different ways. The intermediate states may involve periodic solutions consisting of interacting 3D rarefaction pulses that belong to the lower branch of the Jones-Roberts cusp with  $\mathcal{P} < \mathcal{P}_0$ .

We have performed direct numerical simulations using the numerical method described in [9]. We solve the GP equation in the reference frame moving with the velocity  $U_f$  chosen in such a way that the main disturbance is kept within the computational box:

$$-2i\frac{\partial\psi}{\partial t} + 2iU_f\frac{\partial\psi}{\partial x} = \nabla^2\psi + (1 - |\psi|^2)\psi. \quad (6)$$

In these computations we follow the evolution of the asymptotic solution (5) extended along the  $z$ -axis and moving in the  $x$ -direction. The dimensions of the computational box are  $D_x = 60$ ,  $D_y = 60$ ,  $D_z = 180$ . The  $xy$ -faces of the box are open, to allow sound waves to escape; this is achieved numerically by applying the Raymond-Kuo technique [10]. The  $z = 0$  and  $z = D_z$  sides are reflective.

The soliton (5) was perturbed along the  $z$ -axis, so that at  $t = 0$

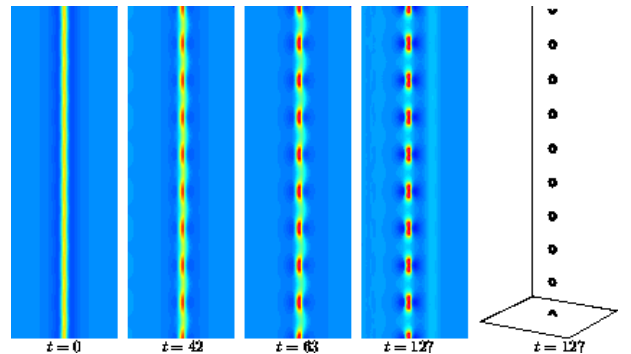
$$x \rightarrow x + 0.1 \cos(kz). \quad (7)$$

We choose  $k$  so that  $N$  periods of this perturbation fit exactly into the  $D_z$  dimension of the box. There are two main parameters of the problem that determine the final outcome of the instability:  $\epsilon$ , which determines the configuration, energy, and momentum of the initial field, and the wavelength of the perturbation  $\ell = D_z/N$ . It can be easily shown using (5) that the energy (2) and the momentum (3) of our initial field per wavelength of perturbation are given by

$$\mathcal{E} = \mathcal{P}/\sqrt{2} = 8\pi\epsilon\ell/3. \quad (8)$$

First, we consider the evolution of the KPI solitary solution subject to large wavelength perturbations  $\ell = 20, 30, 60$  and  $\epsilon = 0.5$ . Fig. 1 illustrates the appearance of vortex rings through contour plots of the cross-section of the solution in the  $xz$ -plane with  $y = D_y/2$  for  $\ell = 20$ . The last panel shows the isosurface  $|\psi|^2 = 0.2$ .

FIG. 1. The contour plot of the density field of the cross-section of solutions of the GP equation. The time snapshots show the evolution of the KPI solution (5) of the GP equation in the  $xz$ -plane with  $y = D_y/2$ . In (5) we took  $\epsilon = 0.5$  and the wavelength of the initial perturbation (7) is  $\ell = 20$ . The last panel shows the isosurface  $|\psi|^2 = 0.2$ . The solutions starting with the third panel possess vorticity and evolve into equally spaced vortex rings.



According to the time snapshots of Fig. 1 the solution evolves directly into a set of vortex rings; other axisymmetric 3D solutions including 3D KPI solitons, are not involved. Moreover, exactly one vortex ring is generated for each wavelength of the perturbation. These vortex rings are distanced  $\ell$  healing lengths apart and have radii much smaller than  $\ell$  (see Table 1). They therefore interact only weakly with each other. The energy and momentum (8) of one period of the perturbation is used to create one vortex ring, the extra energy and momentum escapes and is carried away by sound waves (phonons). The vortex rings are aligned and propagate together with the same velocity. This arrangement of vortex rings is itself unstable and cannot last forever.

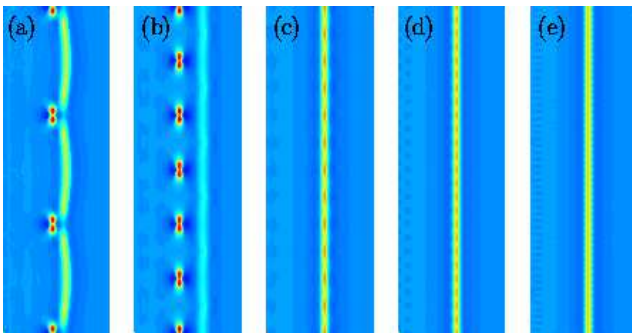
Similar calculations were done for  $\ell = 30$  and  $\ell = 60$ . The results are summarized in Table 1 which gives the energy and momentum per wavelength of the perturbation of the initial field and the energy, momentum, velocity, and radius of the resulting vortex ring.

**Table 1.**

$\ell$	$\mathcal{E}_{\text{init}}$	$\mathcal{P}_{\text{init}}$	$\mathcal{E}_{\text{ring}}$	$\mathcal{P}_{\text{ring}}$	$U_{\text{ring}}$	$R_{\text{ring}}$
60	251	355	99	162	0.45	2.7
30	126	178	86	132	0.49	2.35
20	84	120	71	102	0.53	1.9

Next we explore the evolution of the KPI limit solitary waves of the GP model subject to small wavelength perturbations. The effect of the decrease in the wavelength of the perturbation is twofold: 1) the energy and the momentum (8) per wavelength of the initial field is decreased, therefore leaving less energy available for creating a new entity and 2) these entities are in close proximity to each other so they strongly interact. Fig. 2 plots the cross-sections of the solutions for  $\epsilon = 0.5$  and  $\ell = 60, 30, 15, 7.5, 3.75$ . The first two panels (Fig. 2a and 2b) illustrate the vortex nucleation discussed earlier. To the best of our knowledge the periodic solutions shown on Fig. 2c-e are unknown in the literature on the GP model or the nonlinear Schrödinger equation. The interesting feature of these solutions is that they lack a vorticity and have small energy and momentum per period that tend to zero as  $\ell \rightarrow 0$ . These solutions can be understood as periodic pulse trains composed of the rarefaction pulses positioned on the lower branch of the Jones-Roberts sequence with  $\mathcal{P} < \mathcal{P}_0$ . The interaction between adjacent pulses reduces the total energy per period. The analysis of these and other properties of periodic pulse trains composed from the solitary waves of nonintegrable evolution equations can be found in [11].

FIG. 2. The contour plot of the density field of the cross-section of solutions of the GP equation. The time snapshots show the different stages in the evolution of the KPI-limit solution (5) of the GP equation in the  $xz$ -plane with  $y = D_y/2$ . In (5) we took  $\epsilon = 0.5$  and the wavelengths of the initial perturbation (7) were  $\ell = 60$  (a),  $\ell = 30$  (b),  $\ell = 15$  (c),  $\ell = 7.5$  (d), and  $\ell = 3.75$  (e). The contour plots are shown for  $|\psi|^2$  at  $t = 149$  for (a) and  $t = 127$  for the rest of panels.



Other findings are summarized in Table 2 which gives the values of the energy and momentum of the initial field and the resulting periodic rarefaction solution.

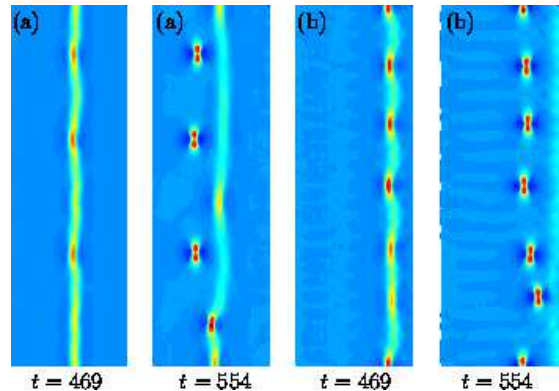
**Table 2.**

$\ell$	$\mathcal{E}_{\text{init}}$	$\mathcal{P}_{\text{init}}$	$\mathcal{E}_{\text{per}}$	$\mathcal{P}_{\text{per}}$
15	62	90	55	78
7.5	31.5	46.2	30.7	44
3.75	15.5	23	15	21

These periodic solutions can execute standing wave oscillations of decreasing amplitude and period  $\ell/2$ . Sim-

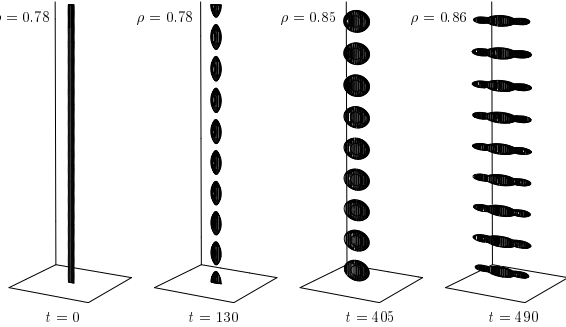
ilarly to the periodic solutions made of aligned vortex rings, the periodic rarefaction solutions become unstable and we followed the development of this instability. Fig. 3a shows the contour plots of the density for a cross-section of the field which evolves from the periodic rarefaction solution with  $\ell = 15$  to produce total of four rings. Therefore, to create each ring the energy and momentum of several periods of the rarefaction solution were used. The wavelength of the secondary instability that destroyed the periodic solution is approximately 57. Similar calculations were done for the even shorter perturbation wavelength  $\ell = 7.5$ ; see Fig. 3b. The wavelength of the secondary instability is approximately 29 resulting in the appearance of six rings. The reason for the apparent nonuniformity of the nucleated rings is that  $D_z$  is not an exact multiple of these wavelengths.

FIG. 3. The contour plot of the density field of the cross-section of solutions of the GP equation. The time snapshots show the different stages in the evolution of the KPI-limit solution (5) of the GP equation with  $\epsilon = 0.5$  in the  $xz$ -plane with  $y = D_y/2$ . The wavelengths of the initial perturbation (7) are  $\ell = 15$  (a) and  $\ell = 7.5$  (b).



Finally, we consider the evolution of the small energy and momentum KPI limit solitary waves. In these computations we use  $\epsilon = 0.3$  and  $\ell = 60, 30, 20, 15$ . For  $\ell = 60$  the KPI solution follows the scenario of vortex nucleation and directly evolves into 3 vortex rings of small radii. For smaller wavelengths  $\ell = 30, 20, 15$  the KPI solution initially evolves into oscillating periodic rarefaction pulses of decreasing  $y$ -extent. The energy and momentum per period are apparently insufficient to allow them to evolve into rings and the necessary energy cannot be reduced through interactions when the putative solutions are separated by such large distances. These solutions break down into sound waves that carry off all energy and momentum; see Fig. 4.

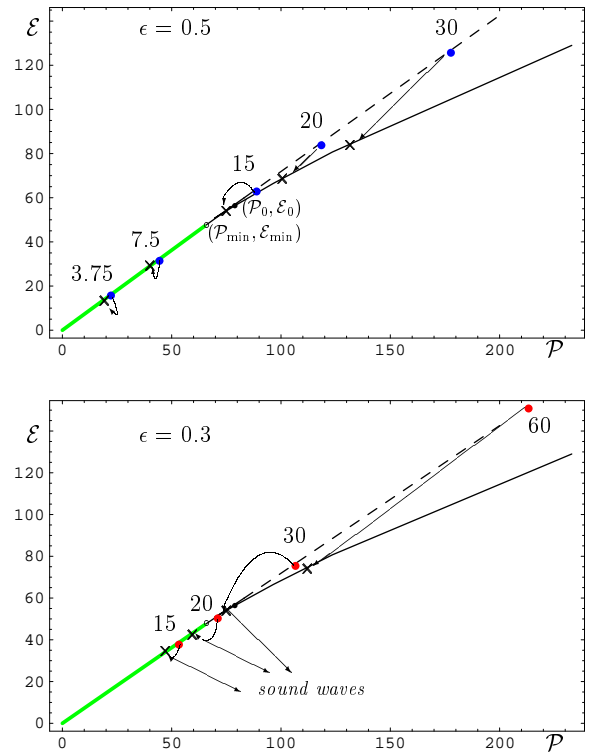
FIG. 4. Isosurfaces of the density field of solutions of the GP equation. The time snapshots show the different stages in the evolution of the KPI-limit solution (5) of the GP equation with  $\epsilon = 0.3$ . The wavelengths of the initial perturbation (7) is  $\ell = 15$ . The minimum density increases with time and approaches unity as the solution breaks down into sound waves.



In summary, we studied the instability of the 2D KPI limit solitary wave solution in the GP equation. The evolution of several types of solutions are considered. We were able to identify three different regimes of transition depending on the initial energy and momentum of the KPI solution and on the wavelength of the initial perturbation. For large wavelengths, the initial solution immediately evolves into a periodic solution consisting of small equally spaced vortex rings with a period equal to the period of the initial perturbation. For shorter wavelengths the KPI solution first evolves into a periodic solution consisting of 3D interacting rarefaction pulses that later break up into vortex rings under the influence of a secondary instability of a different wavelength. Finally, if the energy of the KPI solution is small the solution can break into sound waves after forming an oscillating periodic rarefaction pulse.

Fig. 5 summarizes all calculations performed and the relationships of the different regimes studied. The initial states considered are represented by dots on the  $\mathcal{PE}$ -plane, where  $\mathcal{E}$  and  $\mathcal{P}$  are defined per wavelength of the perturbation. We plot the cusp determined by Jones and Roberts [2] for the family of the vortex rings and rarefaction pulses. The arrows show the way the initial state evolve.

FIG. 5. Summary of numerical integration of (6) starting with the initial condition (5) with  $\epsilon = 0.5$  and  $\epsilon = 0.3$ . The cusp corresponds to the 3D solitary wave solutions. Dashing of the upper branch indicates that this branch is unstable.  $(\mathcal{P}_0, \mathcal{E}_0)$  marks the point where the vorticity disappears and point  $(\mathcal{P}_{\min}, \mathcal{E}_{\min})$  gives the position of the lowest momentum-energy state of the 3D solitary solution (see discussion in the text). The line from the origin to  $(\mathcal{P}_{\min}, \mathcal{E}_{\min})$  corresponds to the family of periodic rarefaction pulses. Dots indicate the position of the initial states, the wavelength of the perturbation  $\ell$  is given next to each initial state; arrows show the evolution of these solutions, and the crosses correspond to the final state before the onset of the secondary instability.



This work was supported by the NSF grants DMS-9803480 and DMS-0104288. The author is very grateful to Professor Paul Roberts for many useful discussions about this work.

---

[1] V.L. Ginzburg and L.P. Pitaevskii, Zh. Eksp.Teor. Fiz. **34**, 1240 (1958) [Sov. Phys. JETP **7**, 858 (1958)]; E.P. Gross, Nuovo Cimento **20**, 454 (1961); L.P. Pitaevskii, Soviet Physics JETP, **13**, 451 (1961).  
[2] C. A. Jones and P. H. Roberts, J. Phys. A: Gen. Phys. **15**, 2599 (1982)  
[3] B.B. Kadomtsev and V. I. Petviashvili, Sov. Phys. Dokl., **15**, 39 (1970)  
[4] S. V. Manakov, V. E. Zakharov, L. A. Bortdag, A. R. Its, and V. B. Matveev, Phys. Lett., **63A** 205 (1977)  
[5] E. A. Kuznetsov and S. K. Turytsin, Sov. Phys. JETP, **55**, 844 (1982)  
[6] E. A. Kuznetsov and J. Juul Rasmussen, Phys. Rev. E, **51**, 4479 (1995)  
[7] N. G. Berloff and P. H. Roberts, submitted to J. Phys. A : Math. Gen., cond-mat/0106547 (2001)  
[8] A. Senatorski and E. Infeld, Phys. Rev. E, **57** 6050 (1998)  
[9] N. G. Berloff and P. H. Roberts, J. Phys.: Math. Gen. **33**, 4025 (2000)  
[10] G. W. Raymond and H. L. Kuo, Q. J. R. Meteorol. Soc., **110** 525 (1984)  
[11] N.G. Berloff and L. N. Howard, Stud. App. Math., **99**, 1 (1997); **100**, 195 (1998)